Morphological Transitions

DOI: 10.1002/anie.201102364

Programmed Morphological Transitions of Multisegment Assemblies by Molecular Chaperone Analogues**

*Job Boekhoven, Aurelie M. Brizard, Patrick van Rijn, Marc C. A. Stuart, Rienk Eelkema, and Jan H. van Esch**

Supramolecular morphological transitions are of great importance in many processes in molecular biology. The Golgi apparatus bilayer, for instance, constantly transforms into cargo vesicles mediated by coaggregation with protein coats,[1] but also proteins fold and unfold by coaggregation with chaperone proteins. In the latter case, chaperones selectively switch off the self-assembly of parts of the protein, thereby controlling their structure and function.[2] Such a strategy can be of use for the development of smart materials, in which an external trigger induces a morphological transition, altering the macroscopic properties of the material.

The use of coaggregation to induce morphological transitions has indeed been applied successfully to artificial systems, hence leading to the development of smart materials. The main strategy so far is to alter the packing parameter of a surfactant[3] leading to morphological changes following the structure–shape concept. By this strategy, the transition of vesicles to hexagonal phases by the addition of trimethylbenzene,[4] the conversions of spheres into rods into tubes by addition of ions[5] as well as other additives[6] have been induced. Other strategies to induce morphological changes have also been applied, for example, the use of two-component gel systems[7] or photoisomerization of the building block.[8] Although in all cases the mechanisms of these morphological transitions are well understood, the outcome can be hard to predict. Therefore, it remains a challenge to program the outcome of such transitions within the initial building block, which is necessary to use this approach for smart materials.

Herein we demonstrate that morphological transitions can easily be programmed by separately addressing the complex aggregation behavior of a segmented self-assembling molecule, using small molecule chaperone analogues, that is, small molecules that selectively switch off self-assembly of another molecule through selective association. As a model system, we use a previously described multisegment amphiphile that consists of two covalently linked but orthogonally self-assembling building blocks, and which forms architectures characterized by each individual segment.[9] Through the addition of a chaperone analogue we can selectively switch off the self-assembly of each of these segments individually, resulting in architectures of the other segment. Interestingly, not only the morphologies of the other segment are retained, but also its dynamics of self-assembly. By such an approach it is possible to design the morphological transitions within the multisegment amphiphile.

The multisegment amphiphile (MA **3**) is constructed of a gelator[10] segment reminiscent of gelator **1** and a surfactant segment reminiscent of EO_4C_8 (surfactant **2**), which assemble orthogonally (Figure 1 a).[11a] We have previously shown that MA **3** in water assembles into architectures that display properties of both parental segments.[9] The gelator segment

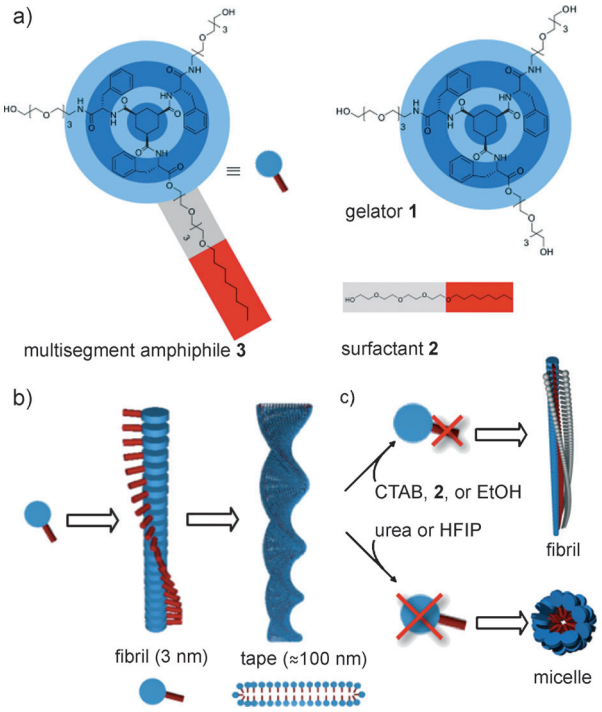

Figure 1. a) Structures of gelator **1**, surfactant **2**, and multisegment amphiphile **3**. b) MA **3** assembles into architectures with properties of both parental building blocks; tapes of hydrogen-bonded fibrils that are held together by hydrophobic interactions. c) By selectively switching off one segment, a morphological transition is brought about, resulting in morphologies of the other segment.

[*] J. Boekhoven, Dr. A. M. Brizard, Dr. P. van Rijn, Dr. R. Eelkema, Prof. Dr. J. H. van Esch
Department of Chemical Engineering
Delft University of Technology
Julianalaan 136, 2628 BL, Delft (The Netherlands)
E-mail: j.h.vanesch@tudelft.nl
Homepage: www.cheme.tudelft.nl/sas
Dr. M. C. A. Stuart
Groningen Biomolecular Sciences and Biotechnology Institute
University of Groningen
Nijenborgh 4, 9747 AG, Groningen (The Netherlands)

[**] This work was supported by the Netherlands Organization for Scientific Research (NWO).

Supporting information for this article is available on the WWW under http://dx.doi.org/10.1002/anie.201102364.

forces these molecules to stack into fibrils because of intermolecular hydrogen bonding and these fibrils assemble into tapes caused by the hydrophobic interactions between the surfactant segments (Figure 1b). These tapes form an entangled network in the solvent leading to turbid gels above a critical gelation concentration (cgc) of 5.0 mM.

We reasoned that, with the appropriate chaperone analogue, the self-assembly properties of each individual segment can selectively be switched off (Figure 1c). By doing so, the properties of the other self-assembling segment remain, hence giving rise to one of the parental architectures; fibers formed by the gelator segment or surfactant architectures formed by the surfactant segment. An agent that breaks hydrophobic interactions such as a surfactant or cosolvent can be used as a chaperone analogue to switch off the surfactant segment. A hydrogen-bond-breaking agent, such as urea or hexafluoroisopropyl alcohol (HFIP),[12] can be used as a chaperone analogue for the gelator segment.

Herein, cetyl trimethyl ammonium bromide (CTAB) and surfactant **2** were used as chaperones to deactivate the surfactant segment of MA **3**. CTAB and **2** are both spherical-micelle-forming surfactants with critical micelle concentrations (cmc) of 0.9 mM and 8.4 mM respectively.[13]

In pure water, MA **3** formed turbid gels above a concentration of 5.0 mM. Addition of surfactant and a heating-cooling cycle led to a gradual decrease of the cgc of MA **3** if the concentration of the surfactant was above its cmc. In the case of 5.0 mM CTAB, a minimum cgc of 2.5 mM MA **3** was obtained and a minimum cgc of 1.4 mM MA **3** was reached in the presence of 30 mM of **2**. Under these conditions, the formed gels were optically transparent (Figure 2 and the Supporting Information). From this point, the cgc increased in the presence of more surfactant. These observations give strong indications that MA **3** coaggregates with micelles of CTAB or surfactant **2**. The most stable coaggregates are obtained at surfactant concentrations for which the cgc of MA **3** is minimal. At these minima, the surfactant to MA **3** ratio is 1.6 and 13 for CTAB and surfactant **2**, respectively. It should be noted that the surfactant concentrations at these points have been corrected for free surfactant, because coassembly of MA **3** and surfactant only occurred above the cmc of the surfactant. This coaggregation results in a morphological change, hence influencing the macroscopic properties of the gels. It should be emphasized that, for both surfactants, the transitions between turbid and transparent gels required a heating-cooling cycle, thus indicating a significant energy barrier between the two states. Nevertheless, the addition of surfactant at room temperature did decrease the turbidity, but on time scales that were in the range of days (see the Supporting Information). This observation indicates that the transition between the turbid and transparent state is spontaneous, albeit very slow.

To investigate whether the observed changes were indeed due to interactions of the surfactant with the surfactant segment of MA **3**, also the influence of the surfactant on gel formation of gelator **1** without the surfactant segment was studied. The cgc of **1** only changed marginally in the presence of up to 100 mM of CTAB or **2** (see the Supporting Information). Most likely **1** assembles orthogonally with surfactants CTAB and **2**, which is in agreement with previous findings.[11a]

To ensure that the morphological transitions of the tapes were not induced by the surfactant aggregates, also ethanol was used as a chaperone analogue to selectively switch off the

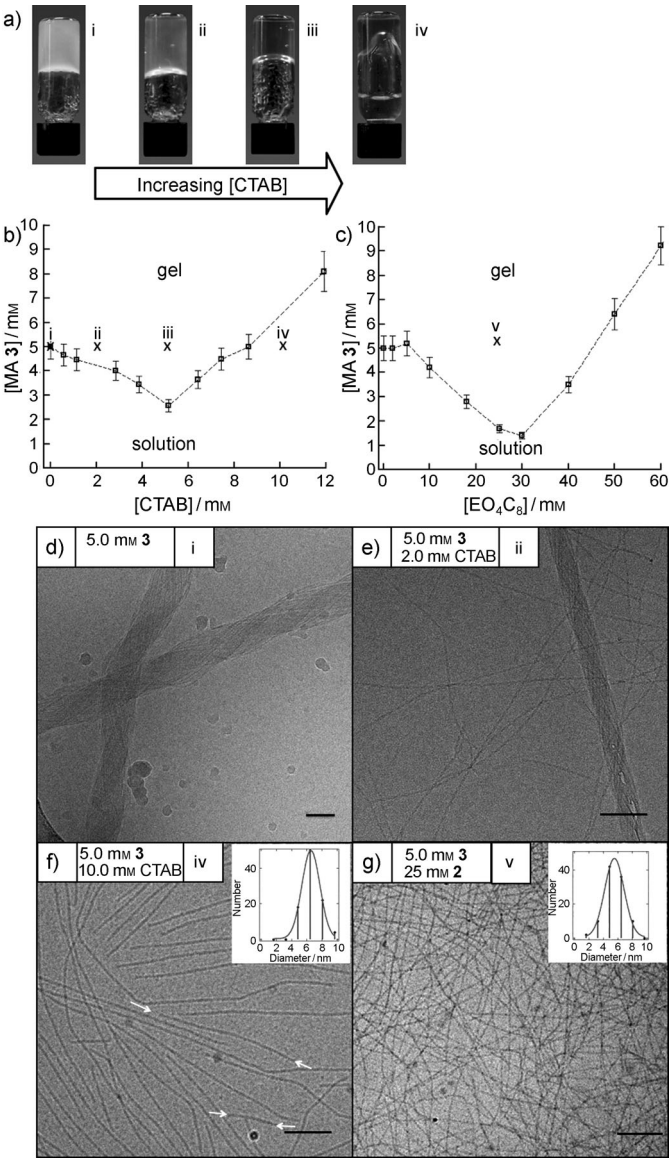

Figure 2. a) Photographs of gels formed by 5.0 mM MA **3** in the presence of 0 mM (i), 2.0 mM (ii), 5.0 mM (iii), and 10.0 mM (iv) CTAB. b) Cgc of complexes formed by MA **3** against [CTAB]. The numbers i–iv refer to the photographs in Figure 2a. c) Cgc of gels of complexes of MA **3** against [**2**]. The error in the cgc determinations is 10% and is indicated by error bars. Cryo-TEM images of: d) gel of MA **3** at 5.0 mM showing twisted tapes with diameters up to 100 nm (i); e) gel of 5.0 mM MA **3** and 2.0 mM CTAB showing both bundles of fibers and smaller 6.6±1 nm fibers (ii); f) gel of 5.0 mM MA **3** and 10.0 mM CTAB showing only 6.6±1 nm fibers (iv), increasing the CTAB concentration leads to the formation of shorter fibers (white arrows); g) gel fibers of 5.0 mM **3** and 25 mM **2** showing 5.5±1 nm fibers (v). The numbers i–v refer to the photographs and cgc data in Figure 2a,b, and c. The insets in Figure 2 f,g show the statistical distribution of fiber diameters and the Gaussian fit. All scale bars are 100 nm.

surfactant segment of MA **3**. Similar to chaperone analogues **2** and CTAB, the turbidity of gels decreased drastically in the presence of 500 mM ethanol (see the Supporting Information). Moreover, in the presence of ethanol also the cgc decreased, from 5 mM to 0.6 mM (Figure 3a).

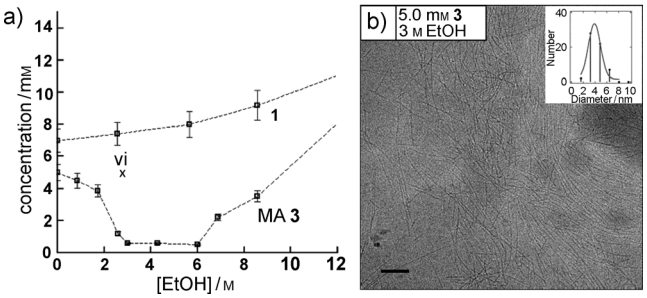

Figure 3. a) Cgc of gels of complexes of MA **3** against EtOH concentration reveals the decrease of the cgc when up to 6 M ethanol is added. EtOH has an inverted effect on the self-assembly of **1.** The error in the cgc determinations is 10%. The number vi refers to the conditions of cryo-TEM image in Figure 3b; b) cryo-TEM image of 5 mM gel of MA **3** in the presence of 3 M ethanol shows fibrils with a monodisperse diameter of 3.9 ± 1 nm. The inset shows the statistical distribution of fiber diameters and its Gaussian fit. Scale bar is 100 nm.

These results strongly indicate that the surfactant segment indeed had been switched off by the chaperone analogues, whereas the hydrogen-bonding interactions between the gelator segments remained unchanged. An FTIR study confirmed that in the presence of CTAB and **2**, the C=O vibrations appeared at wavenumbers characteristic for hydrogen-bonded amides[14] indeed indicating that the hydrogen-bonding interactions were not affected (see the Supporting Information). To confirm that the hydrophobic domains were indeed switched off, fluorescence spectroscopy using the Nile Red solvatochromic probe (NR) was performed.[15] NR in the presence of 1.0 mM MA **3** in water typically showed a blue-shift ($\Delta\lambda_{max} = \lambda_{max} - \lambda_{max}$ background) of $\Delta\lambda_{max} = -36$ nm as compared to NR in pure water, which is due to the hydrophobic domains in MA **3** aggregates. In the presence of chaperone analogue ethanol (3 M), this $\Delta\lambda_{max}$ decreased to -8 nm, thus indicating that the hydrophobic domains in MA **3** aggregates in the presence of ethanol had largely disappeared (see the Supporting Information).

To gain more insight into the mechanism of coaggregation, aqueous systems that contain MA **3** (5.0 mM) and varying concentrations of surfactant (CTAB or **2**) were subjected to a cryo-TEM study (Figure 2d–f). With increasing concentration of CTAB the tapes formed by MA **3** gradually disappeared and instead monodisperse fibers with a diameter of 6.6 ± 1 nm were observed. In the presence of 10 mM CTAB the only observed structures were these thin fibers, which was consistent with the observed change in opacity. It should be noted that dissociation of the twisted tapes into a manyfold of thinner fibers also increased the total number of individual fibers per volume. The higher concentration of fibers explains the observed decrease of the cgc upon addition of CTAB. When the concentration of CTAB was further increased, the average length of these thin fibers decreased, which explains the decrease of the cgc at higher concentrations of CTAB (Figure 2f, white arrows and the Supporting Information).

A similar cryo-TEM study was carried out for the coassembly of MA **3** and surfactant **2**. In the case of 5.0 mM MA **3** and 2.0 mM **2** (below its cmc), twisted tapes were observed that were similar to the twisted tapes in the absence of surfactant. However, at a concentration of 25 mM **2**, the only observed structures were thin 5.5 ± 1 nm fibers, thus indicating similar behavior as observed with CTAB, albeit at higher surfactant concentrations (see Figure 2g). The transparent gels formed in the presence of ethanol were also investigated with cryo-TEM and revealed fibrils with a monodisperse diameter of 3.9 ± 1 nm, which is slightly thinner than the fibers observed for MA **3** in the presence of surfactants **2** and CTAB (Figure 3b).

For both surfactant-MA **3** coaggregates the diameter of the fibril is related to the dimensions of its components. The length of a molecule of MA **3** is approximately 3.5 nm and the length of CTAB, **2**, and ethanol is approximately 2.5 nm, approximately 3 nm, and approximately 0.4 nm, respectively. If MA **3** would stack to form fibrils and the surfactant segment would coaggregate with molecules of CTAB or **2**, the diameter of such a fibril would be roughly 6 nm (Figure 1c), which is consistent with the diameter found by cryo-TEM. For coaggregation with ethanol, a diameter of roughly 4 nm is expected, which is also in agreement with the observed diameter.

At this stage, we wondered if it would be possible to selectively switch off the gelator segment of MA **3** by breaking the intermolecular hydrogen bonds that hold these stacks together. Urea and hexafluoroisopropyl alcohol (HFIP) are well known to disrupt hydrogen bonds in peptides by competing hydrogen-bond formation.[12] In the presence of HFIP (between 0.1 and 0.3 M), MA **3** formed viscous solutions rather than turbid gels and at higher HFIP concentrations, these solutions were transparent (Figure 4a). The transition from opaque to transparent samples indicates that the twisted tapes dissociated into smaller aggregates or single molecules in solution.

Moreover, these morphological transitions invoked by the addition of HFIP took place at room temperature and on a fast time scale; the addition of HFIP to a turbid gel of MA **3** (final concentration of 0.48 M or 5 v/v%) led to the transformation into a transparent solution within 30 seconds. Similar observations were found for the chaperone analogue urea. The addition of urea (final [urea] = 6 M) to a 5 mM gel of MA **3** at room temperature led to the spontaneous transition into a transparent solution within minutes (Figure 4b).

To see if the hydrophobic interactions between the aliphatic tails of the surfactant segment of MA **3** were still present, that is, if urea and HFIP specifically switched off association of the gelator segment, fluorescence spectroscopy using the solvatochromic probe Nile Red (NR) was performed.[15] Solutions of NR in 0.48 M HFIP typically emitted with a λ_{max} of 656 nm, whereas solutions of NR in 6 M urea typically emitted at 660 nm. Increasing the concentration of MA **3** to 0.02 mM led to a $\Delta\lambda_{max}$ of -16 nm in 0.48 M HFIP

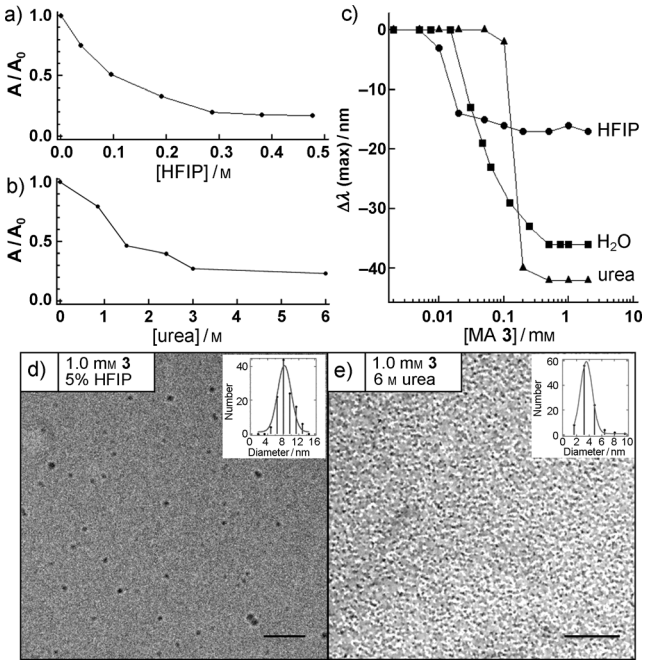

Figure 4. a,b) Normalized absorbance at 500 nm as a measure for turbidity of 1.0 mM MA **3** in water as a function of the HFIP (a) or urea concentration (b). Increasing the concentration of urea or HFIP led to decreasing turbidity. c) $\Delta\lambda_{max}$ of Nile Red fluorescence at different concentrations of MA **3** in water (squares), 0.48 M HFIP (triangles), or 6 M urea (circles). Cryo-TEM images of: d) solution of 1.0 mM in 0.48 M HFIP showing 8.3 ± 1 nm micellar aggregates; e) solution of MA **3** at 1.0 mM in 6 M urea showing 3.9 ± 1 nm micellar aggregates. Inset: statistical distribution of fiber diameters and its Gaussian fit. Scale bars are 100 nm.

solutions; the steady increase in the concentration of MA **3** from 6 M urea to 0.2 mM induced a $\Delta\lambda_{max}$ of −44 nm. In both cases the solutions of MA **3** in HFIP or urea indicate that hydrophobic domains are still present (Figure 4c and the Supporting Information). The abrupt change in NR emission wavelength upon increasing the concentration of MA **3** in 0.48 M HFIP or 6 M urea is indicative of a highly cooperative self-assembly process, which was less pronounced for MA **3** in pure water (Figure 4c). Such a cooperative self-assembly process into hydrophobic domains is typical for self-assembly of amphiphiles, like surfactant **2**.[16] Solutions of gelator segment **1** in urea or HFIP did not display a shift in λ_{max}, thus indicating that **1** does not form hydrophobic domains (see the Supporting Information).

These results point to the fact that the hydrophobic domains remain intact upon addition of these chaperone analogues. In addition, an FTIR study showed a clear shift of the MA **3** C=O vibrations in the presence of HFIP as compared to MA **3** in water. The C=O vibrations appeared at wavenumbers characteristic for amides hydrogen bonded to HFIP[17], thus indicating that HFIP forms competing hydrogen bonds with MA **3** amides and disrupts intermolecular hydrogen bonding between the gelator segments (see the Supporting Information).

A cryo-TEM study revealed that the morphology of the twisted tapes of MA **3** in pure water is strongly affected by the addition of hydrogen-bond-disrupting chaperone analogues. 1.0 mM solutions of MA **3** in pure water displayed similar twisted tapes as samples at 5.0 mM (see the Supporting Information). In the presence of 0.48 M HFIP, solutions of 1.0 mM MA **3** showed micellar aggregates with a diameter of 8.3 ± 1 nm. Solutions of 1.0 mM MA **3** in 6 M urea revealed the presence of micelles with a diameter of 3.9 ± 1 nm. These observations are in good agreement with the observed decrease in opacity as well as the observed cooperative self-assembly behavior (Figure 4d,e).

Dynamic light scattering (DLS) studies of 1.0 mM MA **3** in HFIP revealed the presence of 10 ± 3 nm objects in solution, which is consistent with cryo-TEM (see the Supporting Information). Samples of 1.0 mM MA **3** in 6 M urea did not show a reliable DLS correlation curve, which might be due to a lack of refractive index difference between the solution and the aggregates.

From the results described above we conclude that MA **3** undergoes morphological transitions in the presence of chaperone analogues that selectively switch off self-assembly of one of the two segments. The addition of surfactant as chaperone analogue led to a transition from twisted tapes to thin fibrils, with an elongated morphology reminiscent of the aggregates formed by the parent gelator group. These results led to the conclusion that the surfactants do not affect the hydrogen-bonding capability of the gelator segment, because of the incompatibility of hydrogen bonding and hydrophobic interactions.[11b] However, the surfactants as hydrophobic chaperones compete with the inter-fibril hydrophobic interactions of MA **3**. As a consequence the fibrils do not bundle into twisted tapes, but instead, single fibrils with the surfactant segment shielded by the surfactant molecules are formed (Figure 1c). The elongated shape of these fibrils originates from the strongly anisotropic hydrogen-bonding interactions between the gelator segments.

In contrast, the addition of hydrogen-bond-disrupting chaperone analogues HFIP and urea caused a transition from twisted tapes to small spherical micelles, held together by hydrophobic interactions, and with a morphology reminiscent of spherical micelles formed by the parent surfactant. These results strongly suggest that the urea and HFIP chaperone analogues selectively switch off self-assembly of the gelator segment of this multisegment amphiphile because of competing hydrogen-bonding interactions while preserving the self-assembly properties of the surfactant segment. The directionality of self-assembly of MA **3** is lost because of hydrogen-bond disruption, thus resulting in globular aggregates held together by hydrophobic interactions between the surfactant segments.

Interestingly, not only the morphology but also the time scale of the transition is inherited from the parent segments. In the case of the surfactant chaperones the gelator segment interactions are not affected, and the transition from twisted tapes to single fibrils has a high activation energy with associated long time scales. This observation is nicely in line with the generally slow exchange rates and dynamic properties of hydrogen-bonded hydrogels[6a] like **1**. In contrast, HFIP and urea as chaperones disrupt the hydrogen-bonding interactions between the gelator segments, hence leading to a fast

transition with associated low activation barrier from twisted tapes to micelles. The relatively fast dynamics of this transition compare very well with the dynamic behavior of micellar assemblies that occurrs at millisecond–second time scales.[3]

In conclusion, we have demonstrated that the morphological transitions of a multisegment amphiphile can be programmed in the design of its segments. By addressing an individual segment with a small molecular chaperone analogue, it can be switched off resulting in the formation of architectures associated with the other segment. Interestingly the typical dynamics of self-assembly of each segment are also retained, for example, slow morphological transition for the gelator segment and fast dynamics for the surfactant segment. Such an approach can also be applied to other segmented self-assembling molecules[18], which allows the design of responsive materials in which the morphology of the material before and after addition of chaperone analogues can be programmed; this is a critical aspect for their use as smart materials. Moreover, the ability to program and control morphological transitions and their dynamics by using molecular chaperone analogues will offer new opportunities for the design and construction of hierarchically structured and metastable materials.

Received: April 5, 2011
Revised: June 1, 2011
Published online: July 14, 2011

Keywords: amphiphiles · gelators · morphological transitions · self-assembly · surfactants

[1] J. S. Bonifacino, B. S. Glick, *Cell* **2004**, *116*, 153.
[2] F. U. Hartl, M. Hayer-Hartl, *Science* **2002**, *295*, 1852.
[3] As proposed in: J. N. Israelachvili, D. J. Mitchell, B. W. J. Ninham, *Chem. Soc. Faraday Trans. 2* **1976**, *72*, 1525.
[4] T. Lu, X. Yao, G. Q. Qing Max Lu, Y. He, *J. Colloid Interface Sci.* **2009**, *336*, 368.
[5] L. Zhang, K. Yu, A. Eisenberg, *Science* **1996**, *272*, 1777.
[6] a) *Molecular Gels: Materials with Self- Assembled Fibrillar Networks* (Eds.: R. G. Weiss, P. Terech), Springer, Dordrecht, **2006**, chapter 19.2.2; b) J. Zhu, H. Yu, W. Jiang, *Macromolecules* **2005**, *38*, 7492; c) J. Zhu, N. Ferrer, R. C. Hayward, *Soft Matter* **2009**, *5*, 2471; d) K. T. Kim, J. Zhu, S. A. Meeuwissen, J. J. L. M. Cornelissen, D. J. Pochan, R. J. M. Nolte, J. C. van Hest, *J. Am. Chem. Soc.* **2010**, *132*, 12522.
[7] J. B. Hardy, A. R. Hirst, D. K. Smith, C. Brennan, I. Ashworth, *Chem. Commun.* **2005**, 385.
[8] a) L. Frkanec, M. Jokić, J. Makarević, K. Wolsperger, M. Zinić, *J. Am. Chem. Soc.* **2002**, *124*, 9716; b) S. Kume, K. Kuroiwa, N. Kimizuka, *Chem. Commun.* **2006**, 2442.
[9] J. Boekhoven, P. van Rijn, A. M. Brizard, M. C. A. Stuart, J. H. van Esch, *Chem. Commun.* **2010**, *46*, 3490.
[10] a) A. Aggeli, I. A. Nyrkova, M. Bell, R. Harding, L. Carrick, T. C. McLeish, A. N. Semenov, N. Boden, *Proc. Natl. Acad. Sci. USA* **2001**, *98*, 11857; b) M. George, R. G. Weiss, *J. Am. Chem. Soc.* **2001**, *123*, 10393; c) K. J. van Bommel, C. van der Pol, I. Muizebelt, A. Friggeri, A. Heeres, A. Meetsma, B. L. Feringa, J. van Esch, *Angew. Chem.* **2004**, *116*, 1695; *Angew. Chem. Int. Ed.* **2004**, *43*, 1663; d) A. Del Guerzo, A. G. Olive, J. Reichwagen, H. Hopf, J. P. Desvergne, *J. Am. Chem. Soc.* **2005**, *127*, 17984; e) S. Toledano, R. J. Williams, V. Jayawarna, R. V. Ulijn, *J. Am. Chem. Soc.* **2006**, *128*, 1070; f) F. Rodríguez-Llansola, B. Escuder, J. F. Miravet, *J. Am. Chem. Soc.* **2009**, *131*, 11478.
[11] a) A. Heeres, C. van der Pol, M. Stuart, A. Friggeri, B. L. Feringa, J. van Esch, *J. Am. Chem. Soc.* **2003**, *125*, 14252; b) A. Brizard, M. Stuart, K. van Bommel, A. Friggeri, M. de Jong, J. van Esch, *Angew. Chem.* **2008**, *120*, 2093; *Angew. Chem. Int. Ed.* **2008**, *47*, 2063; c) A. M. Brizard, M. C. A. Stuart, J. H. van Esch, *Faraday Discuss.* **2009**, *143*, 345.
[12] a) I. D. Kuntz, T. S. Brassfield, *Arch. Biochem. Biophys.* **1971**, *142*, 660; b) D. R. Canchi, D. Paschek, A. E. García, *J. Am. Chem. Soc.* **2010**, *132*, 2338.
[13] C. Carnero Ruiz, J. Aguiar, *Mol. Phys.* **1999**, *97*, 1095.
[14] W. D. Jang, T. Aida, *Macromolecules* **2004**, *37*, 7325.
[15] M. C. A. Stuart, J. C. van de Pas, J. B. F. N. Engberts, *J. Phys. Org. Chem.* **2005**, *18*, 929.
[16] M. M. J. Smulders, M. M. L. Nieuwenhuizen, T. F. A. de Greef, P. van der Schoot, A. P. H. J. Schenning, E. W. Meijer, *Chem. Eur. J.* **2010**, *16*, 362. Specific for EO_mC_n surfactants, see ref. [15].
[17] B. B. Doyle, W. Traub, G. P. Lorenzi, F. R. Brown, E. R. Blout, *J. Mol. Biol.* **1970**, *51*, 47.
[18] E. R. Zubarev, M. U. Pralle, E. D. Sone, S. I. Stupp, *J. Am. Chem. Soc.* **2001**, *123*, 4105.

